



# Diffusion of radioactive anion and cation in silver-calcium-bentonite

Noémi M. Nagy<sup>1</sup> · József Kónya<sup>1</sup>

Received: 10 June 2024 / Accepted: 1 November 2024 / Published online: 16 November 2024  
© The Author(s) 2024

## Abstract

In the geological disposal of nuclear waste, the simultaneous reduction of diffusion rate of cationic and anionic radioactive species is essential. Natural calcium-bentonite only reduces the diffusion rate of cations, not anions. In this study, the half of calcium ions in bentonite was exchanged to silver ions to reduce diffusion rates of both of radioactive cation ( $^{137}\text{Cs}^+$ ) and anions ( $^{36}\text{Cl}^-$ ,  $^{131}\text{I}^-$ ) at the same time. This is due to the precipitation of silver halides in the interlayer space. The diffusion rate of both anionic and cationic radioactive species are small in compacted the silver-calcium bentonite.

**Keywords** Diffusion · Mixed silver-calcium-bentonite · Radioactive waste disposal

## Introduction

Recently, a part of the electric energy is produced by nuclear power plants all over the world. However, nuclear power plants produce nuclear waste containing many radioactive isotopes. This waste is deposited in geological repositories [1] safety isolating the nuclear waste from the biosphere as long as 100,000 years. For the storage of radioactive waste, the geological formations were used where water-soluble compounds have been accumulating for millions of years, such as salt mines, clay rocks, granite. In these geological formations, further engineering barriers are constructed.

The isolation ability is characterized by the diffusion rate of the isotopes through the barriers and depends on many factors, including the sorption of radioactive species. Geological formations (natural barriers) are typically able to bind cationic radionuclides due to their negative surface and layer charges, and inhibit their diffusion. However, the sorption of anionic substances can only be ensured with an engineering barrier.

Bentonite clay rock is generally used in any types of waste disposals, and is supposed as barrier material for the deep geological disposal of high activity nuclear waste [2]. The main mineral component in bentonite rocks is

montmorillonite, a swelling clay mineral having exchangeable cations. The radionuclide species, depending on their charges, migrate in the different water spaces of bentonite, namely in the free pore water, the water of the electrostatic double layer, and in the montmorillonite interlayer water [3–6]. The diffusion pathways of the cations and anions are different: the cations can be present in all water types, the anions, however, are excluded from the interlayer water and their quantity is less in the water of the electrostatic double layer than that of cations. The net diffusion coefficient is composed from the diffusion coefficient in the water spaces [7]:

$$D_{\text{tot}} = x_p g_p D_p + x_s g_s D_s + x_i g_i D_i \quad (1)$$

where  $x_p$ ,  $x_s$  and  $x_i$  are the relative quantities of the diffusing ion in the given pathway,  $g_p$ ,  $g_s$  and  $g_i$  are the geometrical factors of the pathways,  $D_p$ ,  $D_s$  and  $D_i$  are the apparent diffusion coefficients on the pathways, p, s and i mean the pore water in the pores, on the outer surfaces and in the interlayer. For anions  $x_i = 0$ .

Moreover, the cations can be sorbed in the interlayer of montmorillonite; this sorption inhibits the diffusion rate of cations. The entity of the interlayer cation highly effects on the swelling of montmorillonite, and as a result the ratio of the water spaces. Many publications deal with the factors influencing the water types, the differences in the diffusion of cations and anions in sodium-bentonite. The diffusion models include the porosity, bentonite dry density, and the distribution coefficient of the migrating cation [8, 9].

✉ Noémi M. Nagy  
nagy.noemi@science.unideb.hu

<sup>1</sup> Imre Lajos Isotope Laboratory, Department of Physical Chemistry, University of Debrecen, Egyetem Tér 1., Debrecen 4032, Hungary

However, the mentioned migration and sorption process can be modified if the cations in the interlayer space of the montmorillonite change to cations that can take place in the chemical reactions of the migrating ion. An example is the precipitation of the interlayer cation and anion, such as the formation of very insoluble precipitates of phosphate or arsenite ion with lanthanide bentonites [10–24]. Another example is the reduction of pertechnetate ions to Tc(IV) by tin(II)- bentonite resulting in the sorption of radioactive pertechnetate [25] and reducing the diffusion rate [6]. Similarly, the precipitation of silver-halides in silver-bentonite is also possible [26]. As a conclusion, anions can also introduce into the interlayer space of montmorillonite and take place in chemical reactions as mentioned before.

In a previous study, we have studied the preparation of silver-bentonite and the batch studies of chloride and iodide ions on this. The calcium-silver ion exchange was proved by X-ray fluorescence and X-ray diffraction studies. Similarly, the precipitation of silver-halogenide was proved by X-ray diffraction. the sorption of radioactive halide ions (iodide and chloride) was studied. It was observed that both anion can be effectively bound with silver-bentonite, so there is a chance that the rate of diffusion can be reduced. However, we have also found that at higher iodide concentrations, the binding of iodide ion is reduced due to the formation of soluble silver-diiodide complexes, thus opening up another diffusion opportunity [26].

In this work, a silver-calcium-bentonite is prepared where half of the montmorillonite layer charge is neutralized by silver ions and the other half by calcium ions. The diffusion of radioactive chloride and iodide anions is studied. The effect of iodide ion concentration on the change in diffusion rate is studied by considering the chemical species. At the same time, the diffusion of the radioactive cesium cation is also being investigated, as the chemical modifications required for anion binding may not result in a significant increase in the diffusion rate of the cation. For this reason, the mixed silver-calcium exchanged bentonite was used for the diffusion studies. This means that a bentonite sorbent is prepared and tested which can simultaneously inhibit the diffusion of anions ( $\text{Cl}^-$  and  $\text{I}^-$ ) by precipitation with silver ions and a cation ( $\text{Cs}^+$ ) taking place in ion exchange reactions with the interlayer cations.

The thermal neutrons of the nuclear reactors produce  $^{36}\text{Cl}$  from  $^{35}\text{Cl}$  in the structural material introduced with the chloride content in the water used for concreting [27]. Due to its long half-life ( $3.01 \times 10^5$  years) it may have a significant long-term effect on human health, because of its long half-life and potential mobility in geosphere.

Radioactive iodine and cesium are products in the fission of  $^{235}\text{U}$  [28] in nuclear reactors. Some radioactive iodine isotopes have very long half-lives, up to  $1.57 \times 10^7$  years ( $^{129}\text{I}$ ). In the aquatic environments [29],  $\text{I}^-$  is the dominant species.

Many different sorbents were found to remove radioactive  $\text{I}^-$ , they are briefly summarized elsewhere [26].

The most important radioactive isotope of cesium ( $^{137}\text{Cs}$ ) is produced with high activity during the fission of  $^{235}\text{U}$  and has relatively long half-life (cca. 30 years) [30]. For this reason, its transport and sorption is frequently studied [31–35].

The typical apparent diffusion coefficient values of the radioactive cations or anion in bentonitic media is in the range of  $10^{-11}$ - $10^{-12}$   $\text{m}^2/\text{s}$  or  $10^{-10}$   $\text{m}^2/\text{s}$ , respectively, but these values strongly depends on the physical and chemical conditions of the migrating solution and the solid matrix [4, 6, 36–41].

## Experimental section

### Materials and chemicals

#### Ca-bentonite

The silver-calcium-bentonite was prepared from calcium-bentonite, collected in Istenmezeje, Hungary, and characterized with respect to its mineralogy and cation exchange capacity (CEC). The raw bentonite was applied without any treatments and purification. The elemental composition of the original Ca-bentonite is: 73.29 mass%  $\text{SiO}_2$ , 18.71 mass%  $\text{Al}_2\text{O}_3$ , 2.98 mass% Fe-oxide, 1.54 mass% CaO and 3.48 mass% MgO. The mineral composition was determined by means of X-ray powder diffraction (XRD) analysis using a Philips PW1710 diffractometer (Philips, (today PANalytical B.V.) De Schakel 18 5651 GH Eindhoven, Netherlands), which is operating at 30 mA and 40 kV using Cu  $\text{K}\alpha$  radiation source and a graphite monochromator. The scanning rate was  $2^\circ/2\theta/\text{min}$ . The mineral composition was calculated on the basis of the relative intensities of the reflections characteristic of the minerals, applying the literature or experimental corundum factors on minerals [42]. The CEC, as determined by the ammonium acetate method [43], was  $8.1 \times 10^{-4}$  eq/g for monovalent cations.

#### Silver-nitrate solution

Silver nitrate solution was prepared from the dissolution of solid  $\text{AgNO}_3$  (Reanal, p.a.). 63.78 g silver nitrate was dissolved in 375  $\text{cm}^3$  tridistilled water. The silver ion concentration of the solution was about 1  $\text{mol dm}^{-3}$ .

#### Radioactive isotopes

The radioactive isotopes ( $^{36}\text{Cl}$ ,  $^{131}\text{I}$ ,  $^{137}\text{Cs}$ ) were purchased from Isotope Institute Ltd, Budapest (Hungary). The iodine and cesium isotopes were carrier-free (concentration  $< 10^{-10}$   $\text{mol/dm}^3$ ) and were present as  $\text{I}^-$  and  $\text{Cs}^+$  ions.

The commercially available  $^{36}\text{Cl}$  isotope contains inactive chloride carrier, the specific activity is 4.8 MBq/g. This means that the chloride concentration of the solution filled into the donor cell (input) (Sect. "Diffusion studies") is about  $1.15 \times 10^{-3} \text{ mol/dm}^3$ .

In nuclear waste the iodine-129 is important because of its very long half-life. In our experiments, however, iodine-131 with short half-life (8 days) was used as a tracer of iodine-129. Their chemical and diffusion properties are just the same.

### Sodium iodide solution

NaI solutions were prepared by dissolving solid NaI (Reanal, puriss) in water. The initial iodide concentrations of the donor cell (input) during the diffusion studies (Sect. "Diffusion studies") varied from  $1 \times 10^{-6}$  to  $5 \times 10^{-4} \text{ mol dm}^{-3}$ .

### Preparation of Ag-Ca-bentonite

Ca-bentonite (120 g, Sect. "Ca-bentonite") was suspended in  $\text{AgNO}_3$  solution ( $375 \text{ cm}^3$ , about  $1 \text{ mol dm}^{-3}$ , Sect. "Silver-nitrate solution"). The suspension was stirred for 5 h at room temperature ( $25 \text{ }^\circ\text{C}$ ), then the suspension was filtered through a  $0.45 \text{ }\mu\text{m}$  pore size membrane filter. The solid was washed by with distilled water until silver ions could be detected in the filtrate by chloride ions. Then the silver-calcium-bentonite was dried in air at room temperature in a silica gel desiccator; the silica gel is changed periodically. Finally, the solid was powdered and homogenized in an agate mortar. During the operations, the bentonite sample was covered by aluminum foil and kept in dark places to avoid the reduction of silver ions to metallic silver due to sunlight.

### Characterization methods

#### X-ray fluorescence measurements

Silver concentration of ion exchanged bentonite was measured using energy dispersive X-ray fluorescence spectroscopy (XRF). Instrumental parameters were: Si(Li) detector with  $20 \text{ mm}^2$  surface and  $3.5 \text{ mm}$  evaporated layer (Atomki, Debrecen, Hungary), Canberra DSA 1000 digital spectrum analyzer (Canberra Industries, Meriden, CT 06450, USA), Canberra Genie 2000 3.0 spectroscopy software (Canberra Industries, Meriden, CT 06450, USA). The sample was excited with  $185 \text{ MBq } ^{241}\text{Am}$  radioactive source. The  $K_{\alpha}$ -lines of silver ( $22.1 \text{ keV}$ ) was used for the measurement. The Ag concentration was  $4.1 \times 10^{-4} \text{ mol g}^{-1}$ . This means that about 50% of the cation exchange capacity ( $8.1 \times 10^{-4} \text{ eq g}^{-1}$ ) was exchanged by silver ions in one ion exchange. Since the original bentonite contained calcium

ions as exchangeable cations, this means that the ratio of silver to calcium ions expressed in equivalent is about 1:1, namely the concentrations of calcium and silver ions is  $2 \times 10^{-4} \text{ mol g}^{-1}$  ( $4 \times 10^{-4} \text{ eq g}^{-1}$ ) and  $4.1 \times 10^{-4} \text{ mol g}^{-1}$ , respectively.

The main mineral component of bentonite is montmorillonite which is a TOT (tetrahedron-octahedron-tetrahedron) type layer silicate. The central ions  $\text{SiO}_4$  tetrahedrons and  $\text{AlOOH}$  octahedrons are the tetravalent Si and the trivalent Al, respectively. In montmorillonite the trivalent aluminum ions are partly substituted by bivalent iron and magnesium ions. This means that the layers become negatively charged, which is neutralized by hydrated calcium ions in the interlayer space between the TOT layers. During the modification by silver ion, only the interlayer cations are exchanged; the central ions of the crystal structure remained unchanged [44].

### Swelling of bentonite

During the study of the swelling of bentonite samples in water, a powder containing 2 g dry bentonite (after the determination of water content) was sprinkled onto the top of  $100 \text{ cm}^3$  of distilled water in a graduated cylinder. The time of bentonite addition was 2 h. After 24 h, the volume of the sediment was measured. This volume was  $14 \text{ cm}^3$ , thus the water introducing into the free pores and interlayer space is  $7 \text{ cm}^3/\text{g}$  silver-calcium-bentonite.

### Measurement of radioactivity

$^{36}\text{Cl}$  was measured on the basis of beta-activity using a Tri-Carb 4810 TR Liquid Scintillation Analyser. The composition of the scintillator was as follows: 4.0 g 1,5-diphenyl-oxazol (PPO),  $257 \text{ cm}^3$  Triton-X 100,  $37 \text{ cm}^3$  ethylene glycol,  $106 \text{ cm}^3$  ethanol, diluted to  $1000 \text{ cm}^3$  with xylene. The samples taken from the receptor half-cells (output) (Sect. "Diffusion studies") were mixed with  $4 \text{ cm}^3$  of this scintillator. Because of the weak beta radiation of  $^{36}\text{Cl}$ , only liquid samples can be well measured, the solid samples activities have significant errors.

The activity  $^{131}\text{I}$  and  $^{137}\text{Cs}$  was measured on the 361 and 662 keV energy gamma lines, respectively, by multi-channel gamma spectrometer equipped with  $\text{NaI(Tl)}$  scintillation detector. Because of the gamma radiation, solid samples obtained by slicing of the bentonite samples (Sect. "Diffusion studies") can also be measured.

The half-lives of the  $^{137}\text{Cs}$  and  $^{36}\text{Cl}$  isotopes are fairly long (30.05 and 301,000 years, respectively), so the activity does not decrease during the studies (about 1 month). The half-life of  $^{131}\text{I}$ , however, is 8 days, so the decay correction of the  $^{131}\text{I}$  was necessary to the starting time to the diffusion studies.

As usual in radioactivity measurement, the background activity was continuously measured and the radioactivities were corrected with this value.

## Diffusion studies

The diffusion cells [45] consisting of three compartments were used. The silver-calcium-bentonite discs with 25 mm diameter and 5 mm thickness is placed in the middle part between two membrane filters (0.45  $\mu\text{m}$  pore size). The pores are bigger by several orders of magnitude than the diameter of the studied ions. In addition, the filter do not adsorb the ions. Thus, the filter do not influence the transport of the radioactive ions. The discs were pressed at about 150 bar pressure, their mass was 4.00 g in the case of disc used for chloride and cesium diffusion studies, or 3.70 g for discs used for iodide diffusion studies, respectively. From the geometric sizes and mass of the disc, the dry density was 1.63  $\text{g}/\text{cm}^3$  (chloride and cesium diffusion) and 1.50  $\text{g}/\text{cm}^3$  (iodide diffusion studies). The bulk density of clay is 2.6  $\text{g}/\text{cm}^3$ . Comparing the dry and bulk densities, the pore ratio is 0.37 or 0.42  $\text{cm}^3/\text{g}$  for the discs used for the study of chloride and cesium, or iodide diffusion, respectively. To avoid the effect of the swelling, mixing, and other processes on the diffusion, the donor half-cell (input) (volume is 55  $\text{cm}^3$ ) and the receptor half-cell (output) (cc. 22.  $\text{cm}^3$ ) was filled with bidistilled water and kept to saturate and swell the bentonite sample. A part of the bidistilled water was taken up by the swelling bentonite, which was shown by the decrease of the water level in the cell; for this reason, the water was filled if necessary. About one month later, the solution in the donor half-cell (input) was exchanged to an initial solution containing the radioactive isotopes. The  $^{137}\text{Cs}$  and  $^{36}\text{Cl}$  isotopes were applied as purchased; this means carrier-free concentration ( $< 10^{-10}$   $\text{mol dm}^{-3}$ ) for cesium and  $1.15 \times 10^{-3}$   $\text{mol dm}^{-3}$  for chloride ions. The diffusion of chloride and cesium ions was also investigated when they were simultaneously present in the donor cell (input). In the case of iodide ion, we tended to study the effect of iodide concentration, thus iodide was applied from carrier-free ( $< 10^{-10}$   $\text{mol dm}^{-3}$ ) up to  $5 \times 10^{-4}$   $\text{mol dm}^{-3}$ . The increase of the concentration was done by non-radioactive NaI solution (Sect. "Sodium iodide solution").

The isotopes migrate through the bentonite layer into the receptor half-cell (output). The samples of 100  $\mu\text{l}$  were taken at different times from the both half-cells. The activity of  $^{36}\text{Cl}$  was measured by its beta activity by liquid scintillation technique.  $^{131}\text{I}$  and  $^{137}\text{Cs}$  isotope emit gamma photons, so their activity was measured by NaI(Tl) scintillation detector (Sect. "Measurement of radioactivity").

After the diffusion experiment was finished (4 weeks) and the cell was disassembled, three discs with 5 mm diameter were cut from the still wet bentonite pastilles. These discs

were sliced into 7 pieces. After air drying, the gamma activities of  $^{131}\text{I}$  and  $^{137}\text{Cs}$  isotopes were measured by gamma spectrometry (Sect. "Measurement of radioactivity").

The diffusion results were evaluated by a particular solution of the Fick's second law:

$$\frac{\partial C}{\partial t} = D_m \frac{\partial^2 C}{\partial x^2} \quad (2)$$

where  $C$  is the concentration of the migrating ion,  $t$  is the time,  $x$  is the distance,  $D_m$  is the apparent diffusion coefficient. For the diffusion cell, the boundary and initial conditions are fulfilled as follows:

boundary condition: at  $x=0$  and  $t>0$ ,  $C=C_0$ ,

initial condition: at  $x>0$  and  $t=0$ ,  $C=0$ .

where  $x=0$  means the contact surface of the solution containing the radioactive solution (donor cell (input)) and the bentonite sample.

In this case, the solution of the Fick's second law [46]:

$$C_{(x,t)} = C_0 \operatorname{erfc} \frac{x}{2\sqrt{(D_m t)}} \quad (3)$$

where  $\operatorname{erfc} z = 1 - \operatorname{erf} z$ ;  $z = \frac{x}{2\sqrt{(D_m t)}}$ .

During the diffusion studies, the radioactive intensities ( $I_{(x,t)}$ ) of the radioactive ions are measured which is proportional to the concentration:

$$I_{(x,t)} = k \lambda V N_A C_{(x,t)} \quad (4)$$

where  $k$  is the measuring efficiency,  $\lambda$  is the decay constant of the radioactive isotopes,  $V$  is the volume of the sample solution,  $N_A$  is the Avogadro number,  $C_{(x,t)}$  is the concentration of the ions. By substituting Eq. (4) into (3):

$$I_{(x,t)} = I_0 \operatorname{erfc} \frac{x}{2\sqrt{(D_m t)}} \quad (5)$$

For the samples taken at different times from the receptor half-cells (output), the apparent diffusion coefficient ( $D_m$ ) can be determined from the function  $C_{(x,t)}-t$  when  $x = \text{constant}$ . The same function is used for sliced samples, but in this case  $t = \text{constant}$ . The results are evaluated with the program "Scientist".

## Results and discussion

### Changes of radioactivity in the solutions of the donor (input) and receptor half-cells (output)

Figure 1 shows the decrease of the radioactivity of the donor half-cells (input) as a function of diffusion time. In Fig. 1a–c, the different notations are the results of parallel experiments. As seen, the depletion of chloride ion from the

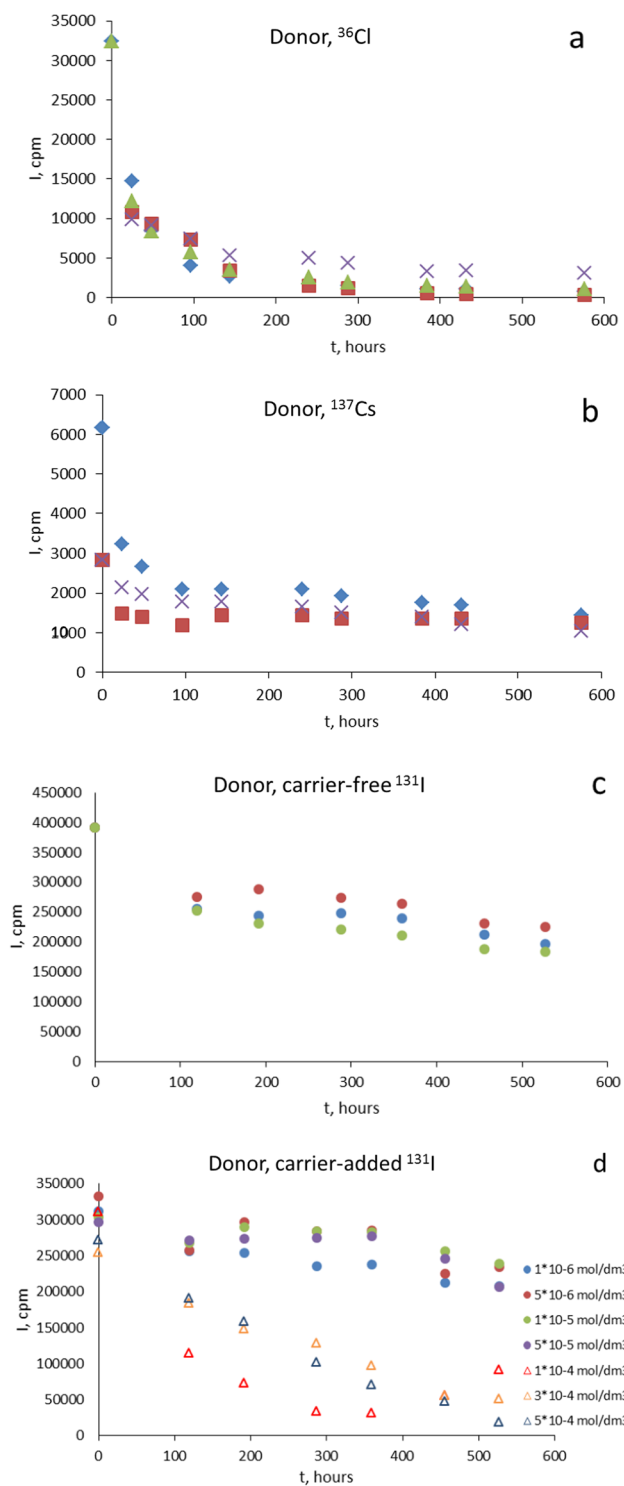


**Fig. 1** The decrease of the radioactivity of the donor cells (input) as a function of migration time. **a:**  $^{36}\text{Cl}$ ; **b:**  $^{137}\text{Cs}$ ; **c:**  $^{131}\text{I}$  at carrier-free concentration; **d:**  $^{131}\text{I}$  at  $1 \times 10^{-6}$ –  $5 \times 10^{-4}$  mol dm $^{-3}$  inactive iodide concentration added

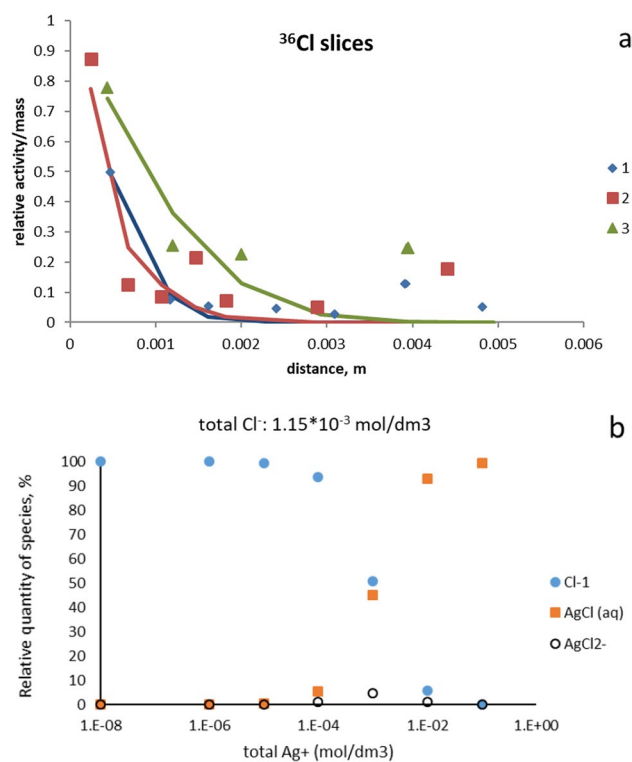


**Fig. 2** **a:** The changes of  $^{36}\text{Cl}$  radioactivity in the bentonite slices. **b:** The chemical species of chloride ions in silver ion-chloride ion system on the basis of thermodynamic calculations. Total chloride concentration:  $1.15 \times 10^{-3}$  mol dm $^{-3}$

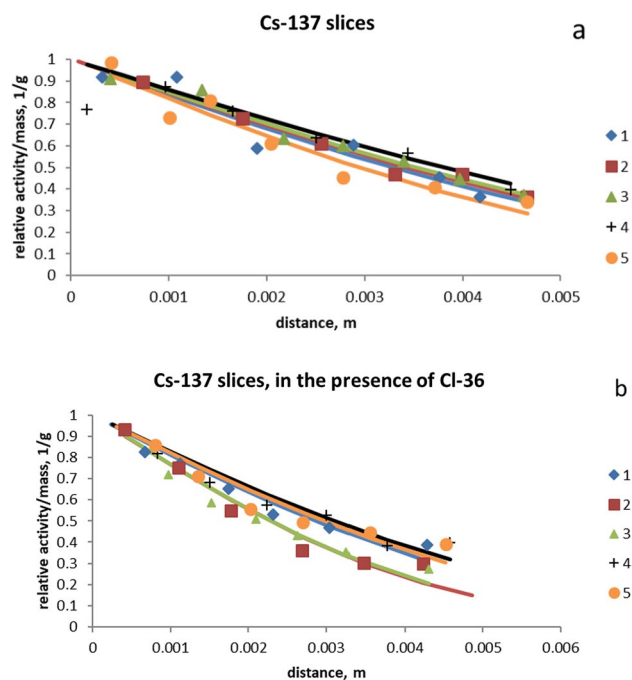


**Fig. 3** The changes of  $^{137}\text{Cs}$  radioactivity in the bentonite slices. **a:** without chloride ion; **b:** with  $1.15 \times 10^{-3}$  mol dm $^{-3}$  chloride concentration

**Table 1** Apparent diffusion coefficients of  $^{36}\text{Cl}$  in silver-calcium bentonite

Sample (Fig. 2a)	$^{36}\text{Cl}$ , $10^{-13} \text{ m}^2/\text{s}$
1	1.15
2	1.77
3	4.20
Mean	2.4
SD	$\pm 1.6$

donor half-cell (input) is the fastest. After about 600 h, the chloride activity of the donor half-cell (input) is less than the 10% of the initial activity. For  $^{137}\text{Cs}$  another high activity remains (about 30% of the initial activity) in the donor half-cell (input) even at long diffusion times.

It is clearly seen in Fig. 1 c and d, the plots belong to three different groups: up to  $5 \times 10^{-5} \text{ mol/dm}^3$  inactive (carrier) iodide concentration, the depletion of  $^{131}\text{I}$  is slower than of the carrier free  $^{131}\text{I}$  isotope. When the inactive iodide concentration is higher than this value, the depletion of iodide from the donor cell (input) is faster than that of the carrier free iodide ion. This means that the iodide concentration strongly affects on the decrease of the radioactivity as well as the iodide concentration in the donor cell (input).

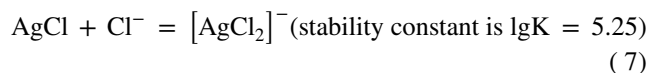
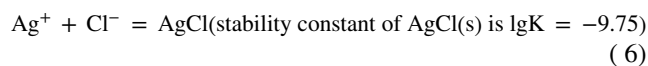
At the same time, no radioactivity is detected in the receptor half-cell (output), consequently diffusion coefficients cannot be calculated from the radioactivities of the receptor half-cells (output) ( $x = \text{constant}$ ). In addition, the radioactivity missing from the donor half-cells (input) must be in the bentonite discs during the experimental period ( $> 600 \text{ h}$ ).

### Changes of radioactivity in the slices of bentonite samples

As mentioned previously in Sect. "Measurement of radioactivity", the  $^{36}\text{Cl}$  isotope emits low energy beta radiation, for this reason the measurement of the solid samples by liquid scintillation method can be measured with significant error. Moreover, in the presence of  $^{137}\text{Cs}$ , which also emit beta particles,  $^{36}\text{Cl}$  cannot be measured at all because of the continuous character of the beta spectra. For this reason, the changes

of  $^{36}\text{Cl}$  radioactivity in the slices can be shown only for cells containing this isotope alone (Fig. 2a). However, the changes of  $^{137}\text{Cs}$  radioactivity can be shown for cells without and with  $^{36}\text{Cl}$  (Fig. 3). Since the initial radioactivities were more or less different for the cells, for the sake of comparison, the relative radioactivities of the slices are plotted, that is all the radioactivity values were divided by the  $I_0$  values obtained during the calculation of diffusion coefficients (Eq. 5). The diffusion coefficients are listed in Table 1 and 2.

As seen in Fig. 2 and Table 1, the diffusion coefficient for  $^{36}\text{Cl}$  are in the range of  $10^{-13} \text{ m}^2/\text{s}$ , which is smaller than the typical values for anion diffusion in natural bentonitic media ( $10^{-10} \text{ m}^2/\text{s}$ ; see Introduction). This can be interpreted by the chemical species of chloride ion in the presence of silver-calcium-bentonite (Fig. 2b). The proportion of chemical forms in the silver-chloride system was calculated using the Visual MINTEQ chemical equilibrium model, using the thermodynamic data of the software [26]:



The diffusion of anions (including chloride) in natural bentonite takes place in the free pore water; they are usually excluded from the interlayer space by electrostatic reasons. In our case, however, the presence of silver ions allows chloride ions to penetrate into the interlayer space. On the one hand, this can open a new diffusion pathway, but it is also possible that silver chloride precipitates, which inhibits the diffusion of chloride. The possibility of the silver chloride precipitation is determined by the ratio of the concentration of silver and chloride ions. This is valid both in the interlayer space and the in the free pore water. The concentration of chloride ions in the cell is  $1.15 \times 10^{-3} \text{ mol dm}^{-3}$  (Sect. "Diffusion studies") and this value was used in the calculations of the chemical species of chloride (Fig. 2b). The concentration of silver ions can be estimated using the following considerations. The amount of silver ions in dry bentonite is  $4.1 \times 10^{-4} \text{ mol g}^{-1}$  (Sect. "X-ray fluorescence measurements"); these ions are located in the interlayer space of bentonite for electrostatic reasons. The pore volume of

**Table 2** Apparent diffusion coefficients of  $^{137}\text{Cs}$  in silver-calcium bentonite

Sample (Fig. 3a)	$^{137}\text{Cs}$ , $10^{-12} \text{ m}^2/\text{s}$	Sample (Fig. 3b)	$^{137}\text{Cs}$ in the presence of chloride, $10^{-12} \text{ m}^2/\text{s}$
1	5.1	1	3.7
2	5.5	2	2.3
3	5.9	3	2.4
4	7.4	4	4.3
5	4.4	5	4.0
Mean	5.6	Mean	3.4
SD	$\pm 1.1$	SD	$\pm 0.94$

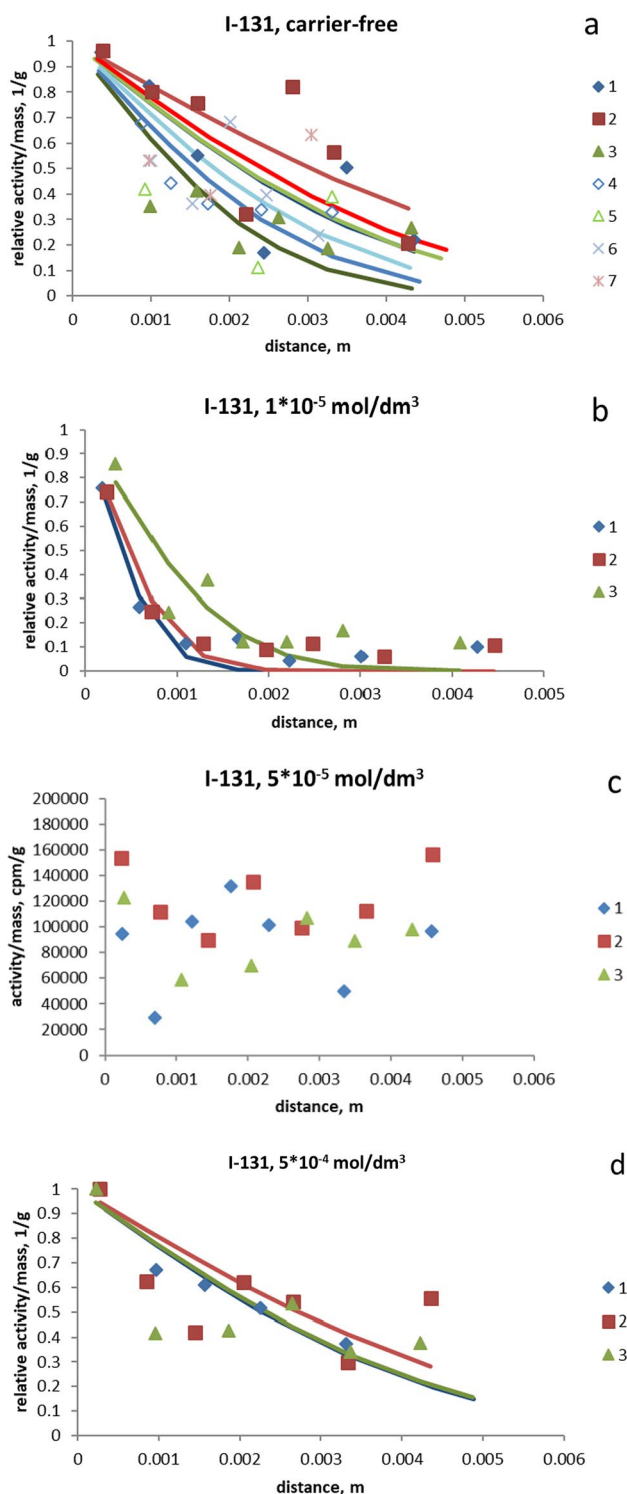


**Fig. 4** The changes of  $^{131}\text{I}$  radioactivity in the bentonite slices. Iodide concentrations: **a**: carrier-free; **b**:  $1 \times 10^{-5} \text{ mol dm}^{-3}$ ; **c**:  $5 \times 10^{-5} \text{ mol dm}^{-3}$ ; **d**:  $5 \times 10^{-4} \text{ mol dm}^{-3}$

the dry bentonite is  $0.37 \text{ cm}^3 \text{ g}^{-1}$  (Sect. "Diffusion studies"), the swelling in water is  $7 \text{ cm}^3 \text{ g}^{-1}$  (Sect. "Swelling of bentonite"). Accordingly, the free pore water volume

is  $0.37 \text{ cm}^3 \text{ g}^{-1}$  and the interlayer water is  $6.63 \text{ cm}^3 \text{ g}^{-1}$ . Taking into account the silver content of the dry bentonite, the silver concentration in the interlayer space is about  $6 \times 10^{-2} \text{ mol dm}^{-3}$ . However, the amount of the free pore water is relatively small (about 5%), thus this does not lead to a significant decrease in the concentration of silver ions in the interlayer space. It should also be noted that silver ions in free pores are subject to much lower electrostatic forces than in the interlayer space, so the concentration of silver ions there can be orders of magnitude lower (at most  $10^{-5}$ – $10^{-4} \text{ mol dm}^{-3}$ ).

Figure 2b shows that at a silver ion concentration of  $10^{-2} \text{ mol dm}^{-3}$  silver ions form a silver chloride precipitate, i.e., the chemical reaction in the interlayer space may be responsible for the lower diffusion coefficient. It is seen, however, that below  $10^{-4} \text{ mol dm}^{-3}$  silver-concentration the dominant chemical species is the negatively charged chloride ion, so its diffusion in the free pore water is still possible. As shown in Fig. 2a and observed during fitting the diffusion model (Eq. 5), the calculated curves fit the measuring points well below about 0.003 m, but not beyond. The presence of chloride ion in the slices above  $\sim 0.003 \text{ m}$  may be due to  $\text{Cl}^-$  diffusion in the free pore water, possibly at higher rates, and may be slightly influenced by the water-soluble  $\text{AgCl}_2^-$  ions, which are also anionic.

Figure 3 and Table 2 show that the parallel experiments for  $^{137}\text{Cs}$  are in a fairly good agreement. The diffusion coefficients are in the range of  $10^{-12} \text{ m}^2/\text{s}$  which is consistent with the literature data (see Introduction). In the presence of chloride ion, which means the formation of silver chloride, the values are a little bit smaller. As a conclusion, the partial ion exchange of the interlayer calcium cations to silver ions, in order to decrease the diffusion rate of anions, does not significantly influence the diffusion of cesium ions.

Figure 4 shows the diffusion of iodide ions from the carrier-free concentration to the addition of  $5 \times 10^{-4} \text{ mol dm}^{-3}$  inactive iodide. The diffusion coefficient values are listed in Table 3.

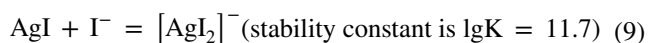
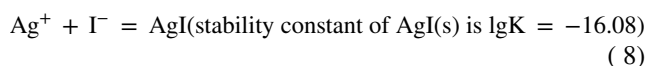
The plots shown in Fig. 4 are selected from the typical run of donor half-cell (input) activities (Fig. 1c and d). Figure 4a shows the carrier-free concentration. Figure 4b indicates an iodide concentration ( $1 \times 10^{-5} \text{ mol dm}^{-3}$ ) where the iodide ion from the donor cell (input) penetrated more slowly into the bentonite pastille than in the case of carrier-free  $^{131}\text{I}$ . Figure 4d shows a case ( $5 \times 10^{-4} \text{ mol dm}^{-3}$ ) where the iodide depletion from the donor cell (input) was faster than that from the carrier-free  $^{131}\text{I}$ . For comparison, relative activities are shown here as in Figs. 2–3. However, the vertical axis of Fig. 4c ( $5 \times 10^{-5} \text{ mol dm}^{-3}$ ) shows activity/mass values, because the slices at this total iodide concentration showed a uniform  $^{131}\text{I}$  activity. Therefore, diffusion coefficients could not be estimated and, in the absence of the fitted curve, the relative activities could not be calculated.

**Table 3** Migration coefficients of  $^{131}\text{I}$  in silver-calcium bentonite

Total iodide, mol/dm <sup>3</sup>	Sample (Fig. 4a)	Migration coefficient, 10 <sup>-12</sup> m <sup>2</sup> /s	Mean 10 <sup>-12</sup> m <sup>2</sup> /s	Standard deviation 10 <sup>-12</sup> m <sup>2</sup> /s
1×10 <sup>-12</sup> (Carrier-free)	1	2.12	2.16	± 1.13
	2	4.22		
	3	0.82		
	4	1.20		
	5	2.33		
	6	1.62		
	7	2.81		
1.00×10 <sup>-06</sup>			1.44*	0.78*
5.00×10 <sup>-06</sup>			0.80*	0.80*
1.00×10 <sup>-05</sup>			0.17*	0.13*
5.00×10 <sup>-05</sup>			uniform distribution	
1.00×10 <sup>-04</sup>			0.16*	0.18*
3.00×10 <sup>-04</sup>			0.09	
5.00×10 <sup>-04</sup>			2.74*	0.56*

\*Mean values of three parallel measurements

The relationship between the diffusion coefficients and the total iodide concentration is shown in Fig. 5a. The value of the diffusion coefficient for the carrier-free iodide concentration is shown by the larger red dot. Figure 5b–d shows the species obtained from the equilibrium calculations for the silver ion concentrations in the interlayer space (10<sup>-2</sup> mol/dm<sup>3</sup>, Fig. 5b) and in the free pore water (10<sup>-5</sup>–10<sup>-4</sup> mol/dm<sup>3</sup>, Fig. 5c, d) of bentonite. The proportion of species in the silver-iodide system was calculated using the Visual MINTEQ chemical equilibrium model, using the thermodynamic data of the software [26]:



It can be seen that at silver concentrations corresponding to the interlayer space (> 10<sup>-2</sup> mol/dm<sup>3</sup>), iodide ions can always be present as AgI precipitates. As a result, the diffusion coefficients at all iodide concentrations are in the range 10<sup>-13</sup>–10<sup>-12</sup> m<sup>2</sup>/s, which is significantly lower than the value typical for anions in natural bentonitic rocks (10<sup>-10</sup> m<sup>2</sup>/s). In turn, the dominant species in the free pore water vary depending on the iodide ion concentration and essentially determine the diffusion rate. These allow us to distinguish here also the concentration ranges where the diffusion rate in the bentonite slices and the rate of iodide transport from the donor cell (input) to the bentonite vary. At the carrier-free iodide concentration, negatively charged iodide ions are present in the free pore water, because the product of the concentration of the ions does not reach the

solubility product required for silver iodide precipitation. However, with the addition of inactive iodide ions, i.e., with an increase in the iodide ion concentration, a silver iodide precipitate is formed and therefore the diffusion rate is reduced compared to the carrier-free iodide ion. This range extends to about 1×10<sup>-4</sup> mol dm<sup>-3</sup> total iodide concentrations. Above this level, the total iodide concentration in the free pores becomes larger than the silver ion concentration and the negatively charged species, I<sup>-</sup> and AgI<sub>2</sub><sup>-</sup> become dominant. This results in the increase of diffusion coefficients.

## Conclusions

About half of the exchangeable ions of natural calcium-bentonite were replaced by silver ions. By this chemical modification, silver-calcium-bentonite was produced. The diffusion rate of the anionic radioactive halide ions in this Ag-Ca-bentonite is 10<sup>-13</sup>–10<sup>-12</sup> m<sup>2</sup>/s, which is significantly lower than the typical diffusion coefficients of anions in natural bentonitic rocks (10<sup>-10</sup> m<sup>2</sup>/s). This is due to the precipitation of silver halides in the interlayer space. At the same time, the rate of diffusion of cationic Cs-137 is also favorably low (10<sup>-12</sup> m<sup>2</sup>/s). This allows a simultaneous reduction of the diffusion rate of both anionic and cationic radioactive species, which is beneficial for the geological disposal of radioactive waste. Silver-calcium-bentonite can be part of the engineering barrier system.

However, it can be observed that in the case of iodide ion, the presence of a carrier influences the species and thus the diffusion rate. The effect depends on the concentration:

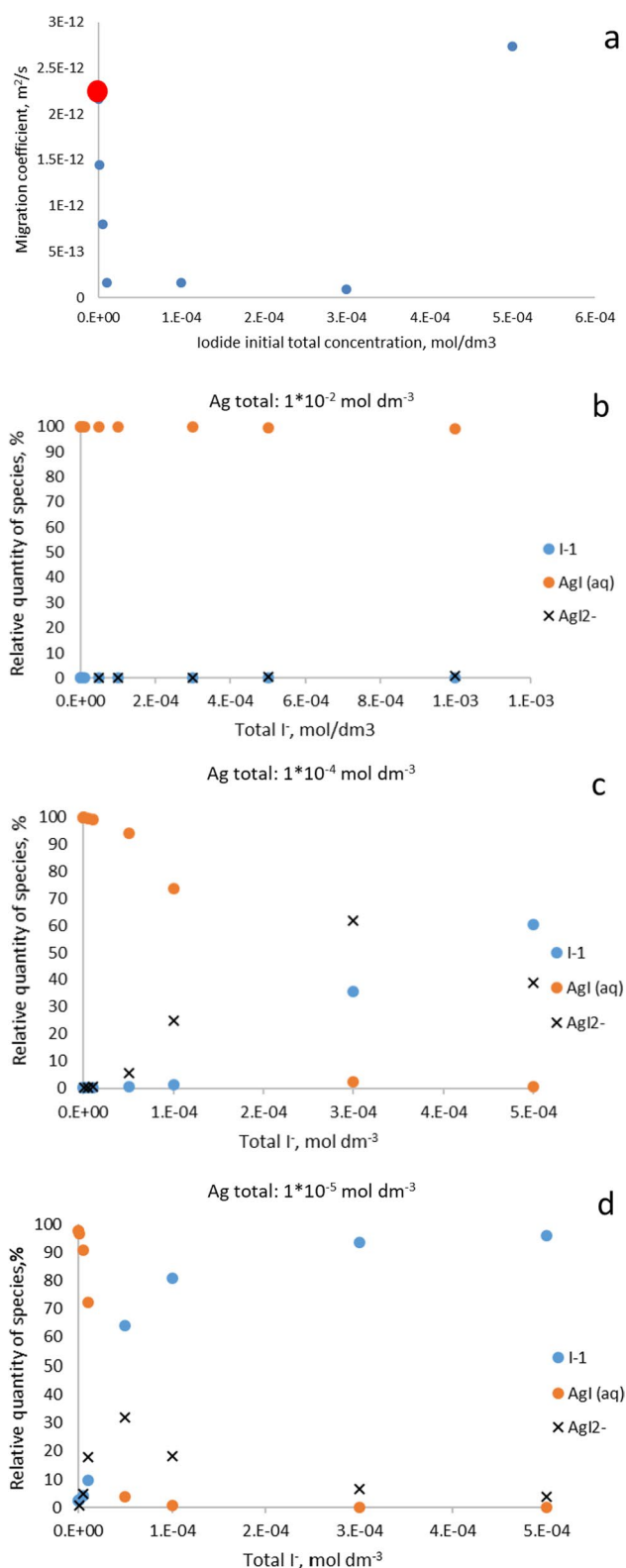


**Fig. 5** **a** The relationship between the migration coefficients and the total iodide concentration. **b–d**: species obtained from the equilibrium calculations for the silver ion concentrations in the interlayer space ( $10^{-2}$  mol/dm<sup>3</sup>, **b**) and in the free pore water ( $10^{-5}$ – $10^{-4}$  mol/dm<sup>3</sup>, **c**, **d**) of bentonite

up to an iodide concentration of about  $10^{-4}$  mol dm<sup>-3</sup>, the diffusion coefficients decrease due to the precipitation of silver iodide. Above this concentration, the diffusion coefficients increase due to the formation of negatively charged  $I^-$  and  $AgI_2^-$  species, but do not increase above the range of  $10^{-12}$  m<sup>2</sup>/s, which is quite appropriate for reducing the diffusion rate of anion.

The silver content of the bentonite layer determines the duration of the diffusion rate reduction. When the silver ions are completely transformed to silver halide, i.e., the silver ions are depleted, the anions can no longer precipitate, so the diffusion rate can increase up to the value typical for anions in natural bentonites. The presence of a carrier therefore has a negative effect, taking some portion of the silver ions up.

**Funding** Open access funding provided by University of Debrecen.

**Open Access** This article is licensed under a Creative Commons Attribution 4.0 International License, which permits use, sharing, adaptation, distribution and reproduction in any medium or format, as long as you give appropriate credit to the original author(s) and the source, provide a link to the Creative Commons licence, and indicate if changes were made. The images or other third party material in this article are included in the article's Creative Commons licence, unless indicated otherwise in a credit line to the material. If material is not included in the article's Creative Commons licence and your intended use is not permitted by statutory regulation or exceeds the permitted use, you will need to obtain permission directly from the copyright holder. To view a copy of this licence, visit <http://creativecommons.org/licenses/by/4.0/>.

## References

- Lavastre V, Jendrzewski N, Agrinier P, Javoy M, Evrard M (2005) Chlorine transfer out of a very low permeability clay sequence (Paris Basin, France): <sup>35</sup>Cl and <sup>37</sup>Cl evidence. *Geochim Cosmochim Acta* 69:4949–4961. <https://doi.org/10.1016/j.gca.2005.04.025>
- Sellin P, Leupin OX (2013) The use of clay as an engineered barrier in radioactive-waste management a review. *Clays Clay Miner* 61:477–498. <https://doi.org/10.1346/CCMN.2013.0610601>
- Bradbury MH, Baeyens B (2003) Porewater chemistry in compacted re-saturated MX-80 bentonite. *J Contam Hydrol* 61:329–338. [https://doi.org/10.1016/S0169-7722\(02\)00125-0](https://doi.org/10.1016/S0169-7722(02)00125-0)
- Van Loon LR, Glaus MA, Müller W (2007) Anion exclusion effects in compacted bentonites: towards a better understanding of anion diffusion. *Appl Geochem* 22:2536–2552. <https://doi.org/10.1016/j.apgeochem.2007.07.008>
- Tournassat C, Appelo CAJ (2011) Modelling approaches for anion-exclusion in compacted Na-bentonite. *Geochim Cosmochim Acta* 75:3698–3710. <https://doi.org/10.1016/j.gca.2011.04.001>
- Shackelford CD, Moore SM (2013) Fickian diffusion of radionuclides for engineered containment barriers: diffusion coefficients, porosities, and complicating issues *Eng Geol* 152:133–147. <https://doi.org/10.1016/j.enggeo.2012.10.014>
- Kozaki T, Liu J, Sato S (2008) Diffusion mechanism of sodium ions in compacted montmorillonite under different NaCl concentration. *Phys Chem Earth* 33:957–961. <https://doi.org/10.1016/j.pce.2008.05.007>

8. Kozaki T, Saito N, Fujishima A, Sato S, Ohashi H (1998) Activation energy for diffusion of chloride ions in compacted sodium montmorillonite. *J Contam Hydrol* 35:67–75. [https://doi.org/10.1016/S0169-7722\(98\)00116-8](https://doi.org/10.1016/S0169-7722(98)00116-8)
9. Molera M, Eriksen T, Jansson M (2003) Anion diffusion pathways in bentonite clay compacted to different dry densities. *Appl Clay Sci* 23:69–76. [https://doi.org/10.1016/S0169-1317\(03\)00088-7](https://doi.org/10.1016/S0169-1317(03)00088-7)
10. Riebe B, Bors J, Dultz S (2001) Retardation capacity of organophilic bentonite for anionic fission products. *J Contam Hydrol* 47:255–264. [https://doi.org/10.1016/S0169-7722\(00\)00154-6](https://doi.org/10.1016/S0169-7722(00)00154-6)
11. Haghseresht F, Wang S, Do DD (2009) A novel lanthanum-modified bentonite, Phoslockm for phosphate removal from wastewaters. *Appl Clay Sci* 46:369–375. <https://doi.org/10.1016/j.clay.2009.09.009>
12. Aghaai MD, Pakizeh M, Ahmadpour A (2013) Synthesis and characterization of modified UZM-5 as adsorbent for nitrate removal from aqueous solution. *Sep Purif Tech* 113:24–32. <https://doi.org/10.1016/j.seppur.2013.04.013>
13. Hacıyakupoglu S, Orucoglu E (2013) Se-75 radioisotope adsorption using Turkey's Resadiye modified bentonites. *Appl Clay Science* 86:190–198. <https://doi.org/10.1016/j.clay.2013.10.010>
14. Hua J (2018) Adsorption of low-concentration arsenic from water by co-modified bentonite- with manganese oxides and poly(dimethylallylammonium chloride). *J Environ Chem Eng* 6:156–168. <https://doi.org/10.1016/j.jece.2017.11.062>
15. Zhu R, Chen Q, Zhou Q, Xi Y, Zhu J, He H (2016) Adsorbents based on montmorillonite for contaminant removal from water: a review. *Appl Clay Science* 123:239–258. <https://doi.org/10.1016/j.clay.2015.12.024>
16. Kamble SP, Dixit P, Rayalu SS, Labhsetwar NK (2009) Defluorination of drinking water using chemically modified bentonite clay. *Desalination* 249:687–693. <https://doi.org/10.1016/j.desal.2009.01.031>
17. Kovács EM, Erdélyiné BE, Kónya P, Kovács-Pálffy P, Harangi S, Kónya J, Nagy NM (2017) Preparation and structure's analyses of lanthanide (Ln)-exchanged bentonites. *Colloid Surf A* 522:287–294. <https://doi.org/10.1016/j.colsurfa.2017.02.085>
18. Cui J, Wang D, Lin J, Wang Y, Ren MY, Shi YP (2021) New application of lanthanum-modified bentonite (Phoslock®) for immobilization of arsenic in sediments. *Environ Sci Pollut R* 28:2052–2062. <https://doi.org/10.1007/s11356-020-10565-x>
19. Li G, Zhang J, Liu J, Chen S, Li H (2020) Investigation of the adsorption characteristics of Cr(VI) onto fly ash, pine nut shells, and modified bentonite. *Desal Water Treat* 195:389–402. <https://doi.org/10.5004/dwt.2020.25909>
20. Yang J, Shi K, Gao X, Hou X, Wu W, Shi W (2020) Hexadecylpyridinium (HDPy) modified bentonite for efficient and selective removal of <sup>99</sup>Tc from wastewater. *Chem Eng J* 382:122894. <https://doi.org/10.1016/j.cej.2019.122894>
21. Yang J, Shi K, Sun X, Gao X, Zhang P, Niu Z, Wu W (2020) An approach for the efficient immobilization of Se-79 using Fe-OOH modified GMZ bentonite. *Radiochim Acta* 108:113–126. <https://doi.org/10.1515/ract-2019-3151>
22. Buzetzy D, Nagy NM, Kónya J (2017) Use of La-, Ce, Y-, and Fe-bentonites for removal phosphate ion from aqueous media. *Period Polytech Chem* 61:27–32. <https://doi.org/10.3311/PPCh.9871>
23. Buzetzy D, Tóth NC, Nagy NM, Kónya J (2019) Application of modified bentonites for arsenite(III) removal from drinking water. *Per Polytechnica Chem Eng* 63:113–121. <https://doi.org/10.3322/PPCh12.197>
24. Buzetzy D, Kovács EM, Nagy NM, Kónya J (2019) Sorption of pertechnetate anion by cation modified bentonites. *J Radioan Nucl Chem* 322:1771–1776. <https://doi.org/10.1007/s10967-019-06852-8>
25. Kovács EM, Buzetzy D, Soha M, Fodor T, Kónya P, Stichleutner S, Kubuki S, Kuzmann E, Kónya J, Nagy NM (2022) Preparation and structure analyses of Sn-bentonite for pertechnetate removal. *Process Saf Environ* 168:133–141. <https://doi.org/10.1016/j.psep.2022.09.075>
26. Buzetzy D, Nagy NM, Kónya J (2020) Use of silver-bentonite in sorption of chloride and iodide ions. *J Radioan Nucl Chem* 326:1795–1804. <https://doi.org/10.1007/s10967-020-07457-2>
27. Sheppard SC, Johnson LH, Godwin BW, Tait JC, Wuschke DM, Davison CC (1996) Chlorine-36 in nuclear waste disposal assessment results for used fuel with comparison to I-129 and C-14. *Waste Manag* 16:607–614. [https://doi.org/10.1016/S0956-053X\(97\)00001-9](https://doi.org/10.1016/S0956-053X(97)00001-9)
28. Buesseler KO, Jayne SR, Fisher NS, Rypina II, Baumann H, Baumann Z, Breier CF, Douglass EM, George J, Macdonald AM (2012) Fukushima-derived radionuclides in the ocean and biota of Japan. *Proc Nat Acad Sci* 109:5984–5988. <https://doi.org/10.1073/pnas.1120794109>
29. MacLean LC, Martinez RE, Fowle DA (2004) Experimental studies of bacteria—iodide adsorption interactions. *Chem Geol* 212:229–238. <https://doi.org/10.1016/j.chemgeo.2004.08.014>
30. McKay HAC (1971) Principles of radiochemistry. Butterworths, London, p 246
31. Bunzl K, Schultz W (1985) Distribution coefficient of Cs-137 and Sr-85 by mixtures of clay and humic material. *J Radioan Nucl Chem* 90:23–37. <https://doi.org/10.1007/bf02037319>
32. Benes P, Stamberg K, Stegmann R (1994) Study of the kinetics of the interaction of Cs-137 and Sr-85 with soil using a batch method—methodological problems. *Radiochim Acta* 66(67):315–321. <https://doi.org/10.1524/ract.1994.6667.special-issue.315>
33. Atun G, Bilgin B, Mardinli A (1996) Sorption of caesium on montmorillonite and effects of salt concentration. *J Radioan Nucl Chem* 211:435–442. <https://doi.org/10.1007/bf02039709>
34. Cho YH, Jeong CH, Hahn PS (1996) Sorption characteristics of Cs-137 onto clay minerals: effect of mineral structure and ionic strength. *J Radioanal Nucl Chem* 204:33–43. <https://doi.org/10.1007/BF02060865>
35. Staunton S, Roubaud M (1997) Adsorption of Cs-137 on montmorillonite and illite: effect of charge compensating cation, ionic strength, concentration of Cs, K and fulvic acid. *Clays Clay Miner* 45:251–260. <https://doi.org/10.1346/CCMN.1997.0450213>
36. Van Loon LR, Baeyens B, Bradbury MH (2005) Diffusion and retention of sodium and strontium in Opalinus clay: Comparison of sorption data from diffusion and batch sorption measurements, and geochemical calculations. *Appl Geochem* 20:2351–2363. <https://doi.org/10.1016/j.apgeochem.2005.08.008>
37. Van Loon LR, Gimmi T, Jakob A, Glaus MA, Diamond LW, Sánchez FG (2008) Self-diffusion of water and its dependence on temperature and ionic strength in highly compacted montmorillonite, illite and kaolinite. *Appl Geochem* 23:3840–3851. <https://doi.org/10.1016/j.apgeochem.2008.08.008>
38. Yaroshchuk AE, Glaus MA, Van Loon LR (2009) Determination of diffusion and sorption parameters of thin confined clay layers by direct fitting of through-diffusion flux. *J Colloid Interface Sci* 337:508–512. <https://doi.org/10.1016/j.jcis.2009.05.049>
39. Glaus MA, Frick S, Rosse R, Van Loon LR (2010) Comparative study of tracer diffusion of HTO, <sup>22</sup>Na<sup>+</sup> and <sup>36</sup>Cl in compacted kaolinite, illite and montmorillonite. *Geochim Cosmochim Acta* 74:1999–2010. <https://doi.org/10.1016/j.gca.2010.01.010>
40. Lee JO, Cho WJ, Choi H (2013) Sorption of cesium and iodide ions onto KENTEX-bentonite. *Environ Earth Sci* 70:2387–2395. <https://doi.org/10.1007/s12665-013-2530-9>
41. Wang C, Myshkin VF, Khan VA, Panamareva AN (2022) A review of the migration of radioactive elements in clay minerals in the context of nuclear waste storage. *J Radioan Nucl Chem* 331:3401–3426. <https://doi.org/10.1007/s10967-022-08394-y>

42. Klug HP, Alexander LE (1954) X-ray diffraction procedures. Wiley, New York
43. Richards LA (ed) (1957) Diagnosis and Improvement of Saline and Alkaline Soils. - U.S. Department of Agriculture, Soil and Water Conservation Research Branch, Agricultural
44. Nagy NM, Kónya J (2022) Interfacial chemistry of rocks and soils, 2nd edn, Taylor and Francis, Boca Raton. ISBN: 9780367856823, pp 272
45. Nagy NM, Kónya J (2013) Chloride ion migration in natural bentonite. *J Radioan Nucl Chem* 298:1519–1526. <https://doi.org/10.1007/s10967-013-2682-9>
46. Crank J (1979) The mathematics of diffusion. Clarendon Press, Oxford

**Publisher's Note** Springer Nature remains neutral with regard to jurisdictional claims in published maps and institutional affiliations.